

# On the Capture of Dark Matter by Neutron Stars

Tolga Güver,<sup>a</sup> Arif Emre Erkoca,<sup>b</sup> Mary Hall Reno<sup>c</sup> and Ina Sarcevic<sup>b,d</sup>

<sup>a</sup>Department of Astronomy and Space Sciences, Faculty of Sciences, Istanbul University, 34119 University, Istanbul, Turkey

<sup>b</sup>Department of Physics, University of Arizona, Tucson, AZ 85704

<sup>c</sup>Department of Physics and Astronomy, University of Iowa, Iowa City, IA 52242

<sup>d</sup>Department of Astronomy and Steward Observatory, University of Arizona, Tucson, AZ 85721

E-mail: [tolga.guver@istanbul.edu.tr](mailto:tolga.guver@istanbul.edu.tr), [aerkoca@gmail.com](mailto:aerkoca@gmail.com),  
[mary-hall-reno@uiowa.edu](mailto:mary-hall-reno@uiowa.edu), [ina@physics.arizona.edu](mailto:ina@physics.arizona.edu)

**Abstract.** We calculate the number of dark matter particles that a neutron star accumulates over its lifetime as it rotates around the center of a galaxy, when the dark matter particle is a self-interacting boson but does not self-annihilate. We take into account dark matter interactions with baryonic matter and the time evolution of the dark matter sphere as it collapses within the neutron star. We show that dark matter self-interactions play an important role in the rapid accumulation of dark matter in the core of the neutron star. We consider the possibility of determining an exclusion region of the parameter space for dark matter mass and dark matter interaction cross section with the nucleons as well as dark matter self-interaction cross section, based on the observation of old neutron stars. We show that for a dark matter density of  $10^3 \text{ GeV/cm}^3$  and dark matter mass  $m_\chi \lesssim 10 \text{ GeV}$ , there is a potential exclusion region for dark matter interactions with nucleons that is three orders of magnitude more stringent than without self-interactions. The potential exclusion region for dark matter self-interaction cross sections is many orders of magnitude stronger than the current Bullet Cluster limit. For example, for high dark matter density regions, we find that for  $m_\chi \sim 10 \text{ GeV}$  when the dark matter interaction cross section with the nucleons ranges from  $\sigma_{\chi n} \sim 10^{-52} \text{ cm}^2$  to  $\sigma_{\chi n} \sim 10^{-57} \text{ cm}^2$ , the dark matter self-interaction cross section limit is  $\sigma_{\chi\chi} \lesssim 10^{-33} \text{ cm}^2$ , which is about ten orders of magnitude stronger than the Bullet Cluster limit.

---

## Contents

<b>1</b>	<b>Introduction</b>	<b>1</b>
<b>2</b>	<b>Conditions for the collapse of neutron star</b>	<b>3</b>
2.1	Chandrasekhar limit	3
2.2	Dark matter accumulation regimes and characteristic times	5
2.2.1	Overview	5
2.2.2	First phase - accumulation of dark matter by neutron star	5
2.2.3	Second phase - energy loss with orbits inside neutron star, neutron scattering dominated	7
2.2.4	The onset of self-capture	8
2.3	Conditions for relativistic dark matter particles	9
<b>3</b>	<b>Evaluation of Capture of Dark Matter Particles by Neutron Stars</b>	<b>10</b>
3.1	Dark matter-nucleon interactions	11
3.2	Dark Matter Self Interactions	12
<b>4</b>	<b>Results and Discussion</b>	<b>15</b>
<b>5</b>	<b>Conclusions</b>	<b>19</b>

---

## 1 Introduction

There is overwhelming evidence for the existence of dark matter in the Universe, from the observation of missing mass in galaxy clusters [1] to the precise measurements of the cosmological baryonic fraction performed by WMAP[2] and BOSS[3]. The possibility that the standard gravitation law needs to be modified to explain the observations with the ordinary visible baryonic matter has recently been ruled out by the Bullet Cluster data [4]. The particle physics interpretation of dark matter requires dark matter particles to be weakly interacting and in thermal equilibrium until the Universe expansion becomes such that particles cannot find each other and their interactions freeze-out. Large-scale structure formation indicates that dark matter particles need to be non-relativistic at the time of freeze-out, i.e., dark matter needs to be “cold.” Measurements of the matter density and its baryonic component imply that the dark matter density contribution is about 25% [5–7].

Since the dark matter density is inversely proportional to the dark matter annihilation cross section at freeze-out, the observed density of dark matter in the Universe today constrains the annihilation cross section in the early Universe, specifically at the time of freeze-out. On dimensional grounds, a dark matter particle with mass in the range of 100 GeV to several TeV with weak scale couplings can have annihilation cross sections of the order of  $\langle\sigma v\rangle_{ann} = 3 \times 10^{-26} \text{ cm}^3 \text{ s}^{-1}$  at the freeze-out, providing a natural explanation for the observed density of dark matter today [5]. There have been recent discussions of the possibility of asymmetric dark matter, where the dark matter particles are not self-conjugate, see for example, Refs. [8–15] and references therein. An initial particle-antiparticle asymmetry ultimately leaves non-annihilating DM particles remaining in the current epoch. This is the case we consider in this paper.

As an astronomical object in the Galaxy rotates around the center in its orbit, it will sweep through the Galactic dark matter halo and eventually capture some of the particles on its way. In time, dark matter particles that are captured may have effects on the observational properties of the astronomical object, which may then be used to constrain the nature of the dark matter [11, 12, 16–37]. In that respect, neutron stars provide a natural laboratory to constrain the properties of dark matter [11, 20–35]. Even though the surface area of a typical neutron star is much smaller than more traditional astronomical objects like the Sun, two properties make neutron stars very efficient in capturing Galactic dark matter particles. First, the immense baryonic density inside a neutron star provides a natural location where there it is very likely that dark matter particles will interact and lose energy. Second, because of the strong gravitational force, it is also almost impossible for a dark matter particle to escape from a neutron star once it loses some of its energy through interactions.

It may be only a matter of time for a neutron star to capture enough number of dark matter particles to affect its observational properties. If the dark matter particles are annihilating, one such effect can be seen in the cooling of an old neutron star. The energy outcome of the annihilation process will result in an increase of the temperature that will remain constant and discernible from other cooling processes in time (see, e.g., Ref. [26]). Calculations of the annihilation effects on the cooling of a neutron star show that the resulting effective temperature of a neutron star would be approximately 3000–10000 K [26], depending on the local dark matter density, and the mass and the radius of the neutron star. However, the emission of blackbody radiation at these temperature peaks at the UV to optical wavelengths, where the Galactic extinction hampers our observational capabilities to obtain precise measurements of the surface temperatures of neutron stars unless they are very close.

Even if the dark matter is not annihilating, under certain conditions, the capture process may still have observable effects. For some values of the local dark matter density, dark matter mass and its interactions with nucleons and amongst themselves, the number of particles may be enough for the dark matter to be relativistic and accumulate to numbers larger than the Chandrasekhar limit. Once dark matter inside a neutron star that has reached the Chandrasekhar limit and reaches the self-gravitating limit, it may collapse into a black hole, which could destroy the whole neutron star. In such a case, even the very existence of neutron stars at certain ages can be used to constrain the properties of dark matter. This has been studied in case when dark matter has interactions with baryonic matter only [11, 20, 26].

Neutron star constraints on non-annihilating dark matter have also been recently studied including perturbative self-interactions via a  $\lambda\phi^4$  interaction [30–33]. The introduction of self-interactions modifies the non-interaction bosonic Chandrasekhar limit, but this is model dependent [32, 38, 39]. We focus here on the effect of dark matter with *strong* self-interactions in the accumulation of dark matter in neutron stars. For spin-0 bosons with a  $\lambda\phi^4$  interaction, we are considering coupling constants well beyond the perturbative regime. Our interest here are very small dark matter-nucleon cross sections, yielding slow dark matter thermalization in the neutron star and large self-interaction cross sections which yield a phase of exponentially increasing  $N_\chi$ . This is a regime not covered in the recent literature.

In the absence of a rigorous Chandrasekhar limit for strongly interacting bosons, we use the minimal non-interaction bosonic Chandrasekhar limit, evaluating the parameter space where  $N_\chi$  is large enough to be both self-gravitating and larger than the Chandrasekhar limit for bosons. We discuss the several stages of dark matter accumulation: first the initial capture, then dark matter energy loss by scattering with nucleons and eventually the onset of self-capture, as a function of time. We find that only for large dark matter densities,  $\rho_\chi \gtrsim 10^3$

GeV/cm<sup>3</sup> and  $m_\chi$  less than tens of GeV, is the dark matter number  $N_\chi$  at  $t_{max} = 10^9$  year large enough to satisfy both the minimal Chandrasekhar limit for bosons and the requirement that the dark matter be relativistic, even for strong self-interactions. Given the relatively rare occurrence of such high local dark matter densities, and the likelihood that any model with self-interactions will increase the minimal limit, the existence of neutron stars does not unambiguously constrain even very strongly interacting asymmetric boson theories.

We start the paper in Section 2 by reviewing the conditions necessary for a neutron star to collapse as it captures dark matter particles for both fermionic and bosonic dark matter. We discuss conditions necessary for dark matter particles to be relativistic as they become captured by the neutron star. We discuss the accumulation regimes and characteristic times, and eventual thermalization of the captured dark matter particles. For bosonic dark matter, we review conditions for self-gravitation and discuss the case when bosonic dark matter forms a Bose-Einstein condensate.

In Section 3, we outline our calculation for the time evolution of the dark matter particles as they get captured by a neutron star. In particular, new here is an evaluation of the effect of a time dependent geometric limit for dark matter self-capture in a neutron star. In Section 3 we summarize our inputs and parameters used in the calculation and give a simple example and rough estimate for the range of dark matter cross sections that would result in providing dominant effects on the increase of the number of captured dark matter particles as evolved in time. We discuss our results in Section 4, followed by conclusions in Section 5.

## 2 Conditions for the collapse of neutron star

### 2.1 Chandrasekhar limit

Our focus is on dark matter collapse to a black hole within a neutron star. As discussed below, thermalization of the dark matter particles is an important feature for fermionic dark matter. Subsequent accumulation to the limit of self-gravity is important if bosons have an impact on neutron star collapse. We begin by reviewing the well-known results for neutron star collapse.

For neutron stars, collapse occurs only when the nucleons are relativistic. The relativistic energy of the neutron star is approximately

$$E \sim -\frac{3}{5} \frac{GN_n^2 m_n^2}{R} + \left(\frac{9}{32\pi^2}\right)^{1/3} N_n^{4/3} \frac{\hbar c}{R}, \quad (2.1)$$

where  $G$  is Newton's constant and  $m_n$  is the neutron mass, and  $N_n$  is the number of neutrons. When the gravitational energy of the neutrons equals the energy due to the relativistic Fermi momentum ( $E = 0$ ), the number of neutrons is determined, independent of the radius  $R$  of the neutron star. Additional neutrons cause collapse into a black hole. The limit on  $N_n$  when  $E = 0$  is the Chandrasekhar limit for neutron stars,

$$N_n^{Ch} \approx \left(\frac{1}{Gm_n^2}\right)^{3/2} \approx 2.2 \times 10^{57}. \quad (2.2)$$

More generally, for fermions with mass  $m_\chi$ , the Chandrasekhar limit is

$$N_f^{Ch} \approx \left(\frac{1}{Gm_\chi^2}\right)^{3/2} \approx 1.8 \times 10^{51} \left(\frac{100 \text{ GeV}}{m_\chi}\right)^3, \quad (2.3)$$

where the interactions with neutrons are neglected. An essential feature in this derivation is that the fermions are relativistic. The average energy of a relativistic fermion contained within a radius  $r$  must satisfy

$$E_f \simeq \frac{N_f^{1/3} \hbar c}{r} > m_\chi c^2 . \quad (2.4)$$

This translates to a requirement that the number of fermions  $N_f$  should be larger than  $N_f^{rel}$ ,

$$N_f \geq N_f^{rel} = 1.6 \times 10^{65} \left( \frac{m_\chi}{100 \text{ GeV}} \right)^3 \left( \frac{r}{10.6 \text{ km}} \right)^3 , \quad (2.5)$$

in order that the fermions are relativistic. The number of neutrons in a neutron star with a typical radius of  $r = R = 10.6$  km and neutron star mass in terms of the solar mass  $M_\odot$ ,  $M = 1.44M_\odot$ , is such that the neutrons are non-relativistic. For dark matter fermions to cause the neutron star to collapse, the requirement for relativistic energies may not be satisfied unless  $r \ll 10.6$  km or the dark matter mass is small compared to  $m_n$ . The typical radius containing most of the dark matter reduces when dark matter is thermalized with neutrons in the neutron star, in which case  $r$  is the thermalization radius  $r_{th}$ , much smaller than the neutron star radius. We return to this below.

For bosonic dark matter, there is no Fermi pressure. The corresponding Chandrasekhar-like limit for bosons, again neglecting the gravitational energy associated with neutrons and self-interactions, is [11]

$$N_b^{Ch} \approx \frac{1}{Gm_\chi^2} \approx 1.5 \times 10^{34} \left( \frac{100 \text{ GeV}}{m} \right)^2 , \quad (2.6)$$

since the kinetic energy per boson is of order  $E \sim \hbar c/r$ , the zero point energy due to the uncertainty principle. This approximate limit is confirmed by a number of approaches to calculating the bosonic version of the Chandrasekhar limit [40]. The introduction of self-interactions modifies this limit for bosons, potentially raising the limit to close to the Chandrasekhar limit for fermions [38, 39], although this is model dependent [32]. More recent discussions with perturbative  $\lambda\phi^4$  and relatively quick dark matter thermalization appear in, for example, Refs. [30–33]. Because we are considering non-perturbative self-interaction cross sections, for this paper, we rely on eq. (2.6) for the Chandrasekhar limit for bosons. As we see below, even with this relatively weak constraint on the number of bosons required to form a black hole, large ambient dark matter densities are required for this limit to be reached.

If the dark matter particles are bosons, they are not relativistic unless they get trapped inside the small region of the neutron star. The requirement for relativistic bosons is that  $E \sim \hbar c/r > m_\chi^2$ , so the relativistic condition is

$$\frac{m_\chi}{100 \text{ GeV}} \frac{r}{10.6 \text{ km}} < 2 \times 10^{-22} . \quad (2.7)$$

After bosonic dark matter is thermalized, it is primarily within a small radius, but that radius is not small enough for eq. (2.7) to be satisfied. A larger dark matter density is required for the bosons to form a black hole in the core of the neutron star. An additional stage of accumulation for bosons occurs when bosons form a Bose-Einstein condensate [11, 20, 27]. Finally, when dark matter density  $\rho_\chi$  is larger than the baryon density  $\rho_b$ , the dark matter is self-gravitating, namely, the baryon density can be neglected. Only during this final stage of collapse when self-gravity dominates is the bosonic dark matter eventually relativistic, a requirement for black hole formation.

## 2.2 Dark matter accumulation regimes and characteristic times

### 2.2.1 Overview

Dark matter accumulation by neutron stars occurs in several stages. The first stage is the capture of the ambient dark matter by the neutron star. Cooling of dark matter through interactions in the neutron star cause the orbital radius of the dark matter to decrease, as dark matter continues to accumulate. Thermalization of dark matter with the neutrons in neutron star, the possibility of formation of a Bose-Einstein condensate, the onset of self-gravity and the potential for the dark matter to coalesce into a black hole are all elements of the evolution of the accumulated dark matter. In this section, we discuss the capture and thermalization of dark matter by neutron stars.

Cooling of the dark matter comes from interactions with neutrons. Energy is transferred to the neutrons, which is then dissipated. To first approximation, we may treat the neutrons as a kind of static background for dark matter accumulation and cooling. Scattering with other dark matter does not promote cooling because there is little dissipation of the dark matter. Energy is transferred between dark matter particles, contributing to dark matter capture, but not to dark matter evaporation from the neutron star. As discussed by Zenter in the Appendix of Ref. [17], evaporation of dark matter particles due to dark matter-dark matter scattering will not occur unless the escape velocity inside the neutron star is comparable to the dark matter velocity at a large distance from the neutron star. A typical value for the large distance dark matter velocity is on the order of  $10^{-3}c$  in our galaxy at our location, small compared to the escape velocity of dark matter in a neutron star.

Name	Value
Solar Mass	$M_{\odot} = 1.98892 \times 10^{33} \text{g}$
Velocity dispersion of DM	$\bar{v} = 220 \text{ km/s}$
Neutron Star Mass	$M = 1.44 M_{\odot}$
Neutron Star Radius	$R = 10.6 \text{ km}$
Average Density of Neutron Star	$\rho_b = 5.7 \times 10^{14} \text{g/cm}^3$
Temperature inside the Neutron Star	$10^5 \text{ K}$

**Table 1.** Constants and parameters used in the results presented here.

### 2.2.2 First phase - accumulation of dark matter by neutron star

The initial accumulation of dark matter by neutron stars occurs with dark matter scattering with nucleons with a cross section  $\sigma_{\chi n}$  and with energy loss of the dark matter of approximately

$$\delta E_{\chi} \simeq \frac{2m_r}{m_n + m_{\chi}} E_{\chi} \quad (2.8)$$

where the average incoming kinetic energy is labeled  $E_{\chi} = \langle T_{\text{in}} \rangle$  and the reduced mass is  $m_r = m_n m_{\chi} / (m_n + m_{\chi})$ . In the constant neutron star density approximation, the average kinetic energy of the dark matter inside the neutron star approximated by a trajectory through the center of the neutron star is [28]

$$\langle T_{\text{in}} \rangle = \frac{4}{3} E_* + E_{\text{orbit}} \quad (2.9)$$

where  $E_* = GMm_\chi/R$  and  $E_{\text{orbit}} = -GMm_\chi/(2a)$  for  $a$  the semimajor axis. This expression follows from the assumption that the density of the neutron star  $\rho_b$  is constant. Following Ref. [28], for  $m_\chi \gg m_n$  the time  $t_1$  for the orbit to be contained within the neutron star radius ( $r_\chi(t_1) = R$ ) is

$$t_1 \sim \frac{3\pi m_\chi R^{3/2} \sigma_{\text{crit}}}{4m_n \sqrt{2GM} \sigma_{\chi n}} \sqrt{m_\chi/m_n} \quad (2.10)$$

where relativistic corrections are neglected and  $\sigma_{\text{crit}} = m_n R^2/M$ . Relativistic corrections will not change the time scale by more than a factor of a few. For a neutron star with the parameters of Table I, this leads to a ‘‘containment time’’

$$\begin{aligned} t_1 &\sim 2.7 \times 10^{-57} \left( \frac{m_\chi}{m_n} \right)^{3/2} \frac{\text{cm}^2}{\sigma_{\chi n}} \text{ yr} \\ &\simeq 2.7 \times 10^{-2} \left( \frac{m_\chi}{m_n} \right)^{3/2} \frac{1}{\sigma_{\chi n,55}} \text{ yr} , \end{aligned} \quad (2.11)$$

where  $\sigma_{\chi n,55} = \sigma_{\chi n}/10^{-55} \text{ cm}^2$ . Other choices of density distribution of neutrons in the NS will not dramatically change  $t_1$ . Note also that the expression for  $t_1$  in eq. (2.10) does not rely on the fact that the accumulation of the dark matter is specifically by a neutron star, only that  $m_\chi > m_n$  and that using the average density of the star is reasonable in the evaluation of  $t_1$  [28].

Special to neutron stars is the effect of the Pauli suppression of scattering. For DM with  $m_\chi > m_n$  incident on the neutron star, with  $t < t_1$ , the characteristic energy is large enough that Pauli blocking does not apply. The Fermi energy  $E_F$  in the zero temperature approximation is

$$E_F = \frac{\hbar^2}{2m_n} (3\pi^2 n_b)^{2/3} , \quad (2.12)$$

where  $n_b$  is the number density of neutrons. For the average neutron density used here, the Fermi energy is 97 MeV, which with  $E_F = p_F^2/2m_n$  determines the Fermi momentum  $p_F \simeq 426 \text{ MeV}$ . Pauli blocking is represented by the factor  $\xi$  which depends on the change in momentum  $\delta p$ ,

$$\xi = \min \left[ \frac{\delta p}{p_F}, 1 \right] . \quad (2.13)$$

For  $m_r \simeq m_n < m_\chi$  and the velocities relevant to this phase,  $\xi = 1$ . After  $t_1$ , Pauli blocking is important.

For  $m_r < m_n$ , the evaluation of  $t_1$  [28] is modified by Pauli blocking even for  $t < t_1$ , so that eq. (2.10) becomes

$$t_1 \simeq \frac{3\pi(m_n + m_\chi)R^{3/2}\sigma_{\text{crit}}}{4m_r\sqrt{2GM}\sigma_{\chi n}\xi} \sqrt{m_\chi/m_n} . \quad (2.14)$$

For this stage of the capture, we can take  $\delta p \simeq \sqrt{2}m_r v_{\text{esc}}(R)$  where the escape velocity at  $r = R$  is  $v_{\text{esc}}(R) = \sqrt{2GM/R} \simeq 0.63c$ . For  $m_\chi = 0.1 \text{ GeV}$ , this gives  $t_1 \sim 0.54 \text{ yr}/\sigma_{\chi n,55}$ .

### 2.2.3 Second phase - energy loss with orbits inside neutron star, neutron scattering dominated

After  $t \sim t_1$ , the sphere of dark matter (the “dark matter sphere”) will have a radius of  $r_\chi < R$ . In this section we discuss the evolution of  $r_\chi$  with time. Again, scattering of DM by neutrons gives a change in kinetic energy,  $\delta E_\chi$ , and as a result, the orbital radius decreases. We assume a circular orbit, as in Ref. [28]. The kinetic energy can be expressed in terms of the orbital radius  $r_\chi(t)$ ,

$$E_\chi = \frac{2\pi}{3} G \rho_b m_\chi r_\chi^2, \quad (2.15)$$

with the time rate of change of the kinetic energy,

$$\frac{dE_\chi}{dt} = -\xi n_b \sigma_{\chi n} v \delta E \quad (2.16)$$

with  $\delta E = 2m_r E_\chi / (m_n + m_\chi)$ . Eqs. (2.15) and (2.16) can be combined to yield

$$\frac{dr_\chi}{dt} = -\frac{4\pi\sqrt{2} m_r^3 n_b^2 \sigma_{\chi n} G r_\chi^3}{3 m_\chi p_F} \quad (2.17)$$

for  $t > t_1$ . The solution is that the radius of the dark matter sphere is

$$r_\chi(t) = R \left( 1 + \frac{8\pi\sqrt{2} m_r^3 n_b^2 \sigma_{\chi n} G R^2 (t - t_1)}{3 m_\chi p_F} \right)^{-1/2} \quad (2.18)$$

$t > t_1$ , before thermalization

for a constant neutron density in the neutron star. As already noted, the cooling which is responsible for the shrinking radius comes from scattering of dark matter with neutrons. Dark matter scattering with accumulated dark matter will not contribute to cooling, so eq. (2.18) only depends on  $\sigma_{\chi n}$ , not  $\sigma_{\chi\chi}$ . Numerically, we find that

$$r_\chi^2(t) \simeq \frac{m_\chi}{m_n} \frac{2.8 \times 10^{10} \text{ cm}^2 \text{ yr}}{\sigma_{\chi n,55} t} \quad m_\chi \gg m_n, \quad (2.19)$$

$$r_\chi^2(t) \simeq \frac{m_n^2}{m_\chi^2} \frac{2.8 \times 10^{10} \text{ cm}^2 \text{ yr}}{\sigma_{\chi n,55} t} \quad m_\chi \ll m_n. \quad (2.20)$$

$$(2.21)$$

The next phase in dark matter accumulation may include a significant time in which  $\chi - \chi$  scattering dominates  $\chi - n$  scattering. Since only  $\chi - n$  scattering is relevant to cooling, we can already evaluate the thermalization time. The thermal radius  $r_{th} = r_\chi(t_{th})$  is related to the neutron star temperature  $T$  in the core via

$$E_\chi = \frac{2\pi}{3} G \rho_b m_\chi r_\chi^2(t_{th}) = \frac{3}{2} kT. \quad (2.22)$$

With the solution for  $r_\chi(t)$  in eq. (2.18) at  $t = t_{th}$ , for  $t_{th} \gg t_1$ , one recovers the usual expression (see, e.g., eq. (19) in Ref. [11]),

$$t_{th} = \frac{m_\chi^2 p_F}{6\sqrt{2} T m_n^2 n_b \sigma_{\chi n}} \cdot \frac{m_n^3}{m_r^3} \quad (2.23)$$

$$\simeq 2.5 \times 10^5 \text{ yr} \left( \frac{m_\chi}{m_n} \right)^2 \left( \frac{m_n}{m_r} \right)^3 \frac{1}{\sigma_{\chi n,55}},$$

for  $T = 10^5$  K, a constant neutron star density and  $m_\chi > m_n$ . Numerically, the thermal radius is

$$r_{th} = \left( \frac{9kT}{4\pi G\rho_b m_\chi} \right)^{\frac{1}{2}} = 334 \text{ cm} \left( \frac{m_n}{m_\chi} \right)^{\frac{1}{2}} \quad (2.24)$$

#### 2.2.4 The onset of self-capture

For some sets of parameters, the third phase of dark matter capture by the neutron star comes from the effects of dark matter interactions with the dark matter already captured by the neutron star. In the next section, we discuss the form of the neutron capture and self-interactions of dark matter for the number of accumulated dark matter particles  $N_\chi(t)$ . The neutron capture of dark matter depends on the cross section and number of target neutrons  $N_n$  via  $\sigma_{\chi n} N_n$  while the self capture term for  $dN_\chi/dt$  depends on the self-interaction cross section and the number of already accumulated dark matter particles  $N_\chi$  via  $\sigma_{\chi\chi} N_\chi$ . When self-capture dominates, the linear growth of  $N_\chi(t)$  changes to an exponential growth. We label the time at which the dark matter begins to accumulate exponentially by  $t_2$ .

When the target dark matter is effectively at rest, the change in DM kinetic energy from  $\chi\chi$  scattering is

$$0 \leq \frac{\delta E_\chi}{E_\chi} \leq 1 . \quad (2.25)$$

The kinetic energy of a dark matter particle within the neutron star at orbital radius  $r_\chi$  is

$$E_\chi = \frac{2\pi}{3} G\rho_b m_\chi r_\chi^2 = \frac{1}{4} m_\chi \left( v_{esc}(R) \frac{r_\chi}{R} \right)^2 , \quad (2.26)$$

and  $\delta E_\chi \sim 0.5E_\chi$  for  $\chi\chi$  scattering, neglecting the recoil of the DM that resides in the neutron star. Recoil is important when evaporation of dark matter particles is a possibility. As discussed in Ref. [17], the recoils can be neglected when the dark matter escape speeds are significant compared to the average speed of the (neutron) star and the velocity dispersion in the dark matter halo. The escape speed on the surface of a neutron star is of order  $0.6c$ , and the escape speed increases as the dark matter goes further into the interior of the neutron star. By comparison, the solar speed in the galaxy is on the order of 220 km/s and the DM velocity dispersion is 270 km/s, several orders of magnitude smaller than the dark matter escape speed. Therefore, we can use eq. (2.18) for the radius of the wimp-sphere as a function of time, even when  $\chi\chi$  scattering is important.

An exponential increase in the number of dark matter particles as a function of time because of self-interactions makes the formation of a black hole from dark matter a possibility, even in the regime of slow thermalization considered here. There is an important mitigating effect, however, coming from the geometric limit. The exponential growth of  $N_\chi(t)$  is cut off when the geometric limit is reached,

$$N_\chi(t_G) \sigma_{\chi\chi} = \pi r_\chi^2(t_G) , \quad (2.27)$$

where  $t_G$  is the time at which eq. (2.27) is satisfied. In practice, the thermalization time occurs before  $t_G$  for some parameter choices, in which case eq. (2.18) does not apply after  $t > t_{th}$ .

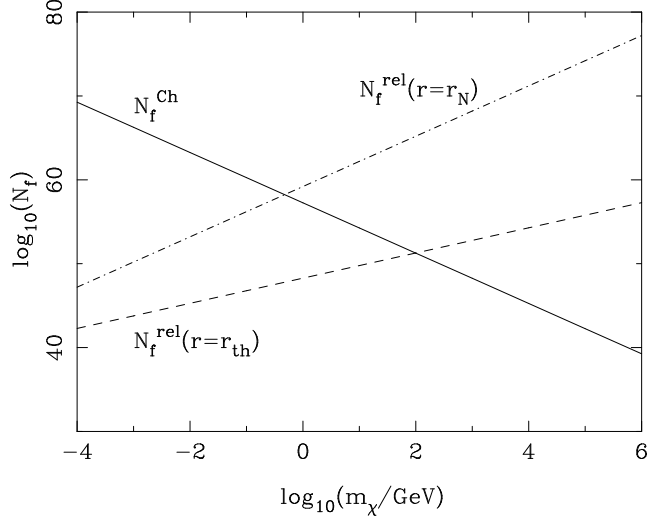


**Figure 1.** As a function of fermionic dark matter  $m_\chi$ ,  $\log_{10}$  of the number of fermions for the Chandrasekhar limit (which requires the dark matter to be relativistic) shown with the solid line and the minimum number of fermions required for relativistic energies when  $r = R$  (dot-dashed) and  $r = r_{th}$  (dashed).

### 2.3 Conditions for relativistic dark matter particles

With thermalization, for fermionic dark matter, one can use  $r_{th}$  in eq. (2.5) to find that

$$N_f \geq N_f^{rel}(r = r_{th}) = 1.9 \times 10^{51} \left( \frac{m_\chi}{100 \text{ GeV}} \cdot \frac{T}{10^5 K} \right)^{3/2}, \quad (2.28)$$

in order for fermionic dark matter to be relativistic. For  $T = 10^5 K$ , the Chandrasekhar limit for fermions, which requires relativistic particles, is applicable only for dark matter masses below 100 GeV when  $t > t_{th}$ , since for  $m_\chi < 100 \text{ GeV}$ ,  $N_f^{Ch} > N_f^{rel}$ . When  $m_\chi > 100 \text{ GeV}$ , fermionic dark matter within the thermal radius with  $N_f = N_f^{Ch}$  is non-relativistic. This appears not to have been taken into account in Ref. [29].

Fig. 1 shows the relevant  $N_f$  for the Chandrasekhar limit, for  $N_f^{rel}(r = r_{th})$  and the number of fermions required for relativistic fermions when  $r = R$ , the radius of the neutron star. Before the thermalization time, the larger of  $N_f^{Ch}$  and  $N_f^{rel}(r = R)$  determines whether or not the dark matter fermions collapse to a black hole. For  $t > t_{th}$ , it is the maximum of  $N_f^{Ch}$  and  $N_f^{rel}(r = r_{th})$ .

If the dark matter particles are bosons, there are additional stages of accumulation of dark matter particles. Within the thermalization radius, as the number of bosons continues to increase in time, the bosons can further form a Bose-Einstein condensate (BEC) [20]. The particle number density required to form a BEC in a sphere of radius  $r_{th}$  in the neutron star is [20, 27]

$$N_b^{BEC}(r = r_{th}) = 2.7 \times 10^{36} \left( \frac{T}{10^5 K} \right)^3. \quad (2.29)$$

Once the BEC forms, the radius in which the dark matter particle can reside, which is the radius of the wave function of the ground state in the gravitational potential of the neutron

star becomes even smaller than  $r_{th}$  [11, 20, 27], namely,

$$\begin{aligned} r_{BEC} &= \left( \frac{3}{8\pi G m_\chi^2 \rho_b} \right)^{1/4} \\ &= 1.5 \times 10^{-5} \text{ cm} \left( \frac{100 \text{ GeV}}{m_\chi} \right)^{1/2}. \end{aligned} \quad (2.30)$$

Clearly,  $r_{BEC} < r_{th}$ , which has significant implications for reaching the Chandrasekhar limit in less time.

If the dark matter particles are bosons, they can only become relativistic and collapse if they become self-gravitating. This happens when the density of the dark matter particles exceeds the baryon density within the same volume. Since the nucleon density does not change in time in the neutron star, as soon as the number of dark matter particles reaches a critical number, the bosons become self-gravitating. This critical number is given by

$$N_{self} = \left( \frac{4\pi r^3 \rho_b}{3m_\chi} \right). \quad (2.31)$$

For  $r = r_{th}$ ,

$$N_{self}(r = r_{th}) \simeq 4.8 \times 10^{46} \left( \frac{1 \text{ GeV}}{m_\chi} \right)^{5/2} \left( \frac{T}{10^5 \text{ K}} \right)^{3/2}. \quad (2.32)$$

Clearly, as the radius of the dark matter core decreases, the condition for the dark matter particles to become self-gravitating will be easier to reach, which would eventually cause the dark matter core to collapse and form a black hole. When the Bose-Einstein condensate has formed,

$$N_{self}(r = r_{BEC}) \simeq 1.1 \times 10^{28} \left( \frac{1 \text{ GeV}}{m_\chi} \right)^{5/2}. \quad (2.33)$$

Comparing the equations for  $N_b^{Ch}$  (eq. (2.6)) and for self-gravitation in eq. (2.32) one can see that the Chandrasekhar limit is already exceeded for thermalized bosonic dark matter when self-gravity is established, as shown in Fig. 2. Self-gravity results in further in-fall and ultimately relativistic bosons, the final requirement for Eq. (2.6) to apply.

To summarize, the necessary condition for collapse of neutron star to a black hole is that the dark matter is thermalized within the age of the neutron star, which we take to be  $10^9$  years. Additionally, in the absence of a specific calculation of the Chandrasekhar limit for bosons with strong self-interactions, we require the number of captured dark matter particles to exceed the following limits:  $N_b^{Ch}$  for  $m_\chi < 7.4 \text{ GeV}$ ,  $N_b^{BEC}$  for  $7.4 \text{ GeV} < m_\chi < 1.26 \times 10^4 \text{ GeV}$ , and  $N_{self}(r = r_{th})$  for  $m_\chi > 1.26 \times 10^4 \text{ GeV}$ .

### 3 Evaluation of Capture of Dark Matter Particles by Neutron Stars

The time evolution of the dark matter particles captured by a neutron star is given by [17]

$$\frac{dN_\chi}{dt} = C_c + C_s N_\chi - C_a N_\chi^2, \quad (3.1)$$

where  $C_c$  is the capture rate due to dark matter-nucleon interactions,  $C_s N_\chi$  is the capture rate due to the dark matter self-interactions and  $C_a N_\chi^2$  governs the number of particles lost

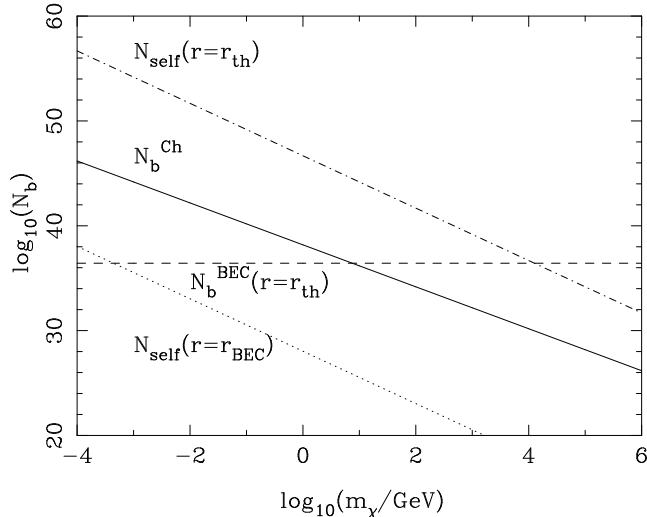


**Figure 2.** As a function of bosonic dark matter  $m_\chi$ ,  $\log_{10}$  of the number of bosons for the Chandrasekhar limit (which requires the dark matter to be relativistic) shown with the solid line, the minimum number of bosons required for the bosons to be self-gravitating when  $r = r_{th}$  (dot-dashed) and  $r = r_{BEC}$  (dotted), and the number of bosons within the radius  $r = r_{th}$  for a Bose-Einstein condensate to form (dashed).

due to their annihilation. We consider the case of asymmetric dark matter, when dark matter particles do not annihilate, so  $C_a = 0$ . In this case, for time-independent  $C_c$  and  $C_s$ , the solution for the eq. (3.1) is

$$N_\chi^0 = \frac{C_c}{C_s} (e^{C_s t} - 1). \quad (3.2)$$

Here the notation  $N_\chi^0$  (rather than  $N_\chi$ ) is to indicate that this is the solution when  $C_c$  and  $C_s$  are time independent. We consider times up to  $t_{max} = 10^9$  yr.

The dark matter self interaction cross section  $\sigma_{\chi\chi}$  enters linearly in  $C_s$ , as discussed below in Sec. 3.2. As noted above, when  $N_\chi \sigma_{\chi\chi} > \pi r_\chi^2$ , the geometric cross section for  $\chi\chi$  scattering in the neutron star, both eq. (3.1) and eq. (3.2) are modified. These modifications are outlined in Sec. 3.2, and we show an example of how the geometric limit on  $\chi$  interactions with the DM in the neutron star affects the growth of  $N_\chi$  as a function of time.

### 3.1 Dark matter-nucleon interactions

The number of dark matter particles that can be captured by a neutron star is given by [26]

$$C_c = \frac{8}{3} \pi^2 \frac{\rho_\chi}{m_\chi} \left( \frac{3}{2\pi\bar{v}^2} \right)^{3/2} \frac{GMR}{1 - \frac{2GM}{R}} \bar{v}^2 (1 - e^{-3\epsilon_0/\bar{v}^2}) \times \xi \text{ f particles s}^{-1}, \quad (3.3)$$

where the general relativistic effects assuming a Schwarzschild geometry have been incorporated. Here  $\rho_\chi$  is the dark matter density at the location of the neutron star,  $m_\chi$  is the mass of the dark matter particles,  $M$  and  $R$  are the mass and the radius of the neutron star, respectively, and  $\bar{v}$  is the average velocity of dark matter particles in the Galactic halo [18] and  $\xi$  is the Pauli blocking factor defined in eq. (2.13). For a dark matter particle to be trapped with a single collision,  $E < m_\chi \epsilon_0$ , which defines  $\epsilon_0$ . Since  $\epsilon_0 \gg \bar{v}^2/2$  we take  $e^{-3\epsilon_0/\bar{v}^2} \simeq 0$

[26]. In order for a dark matter particle to stay inside a neutron star it must lose enough energy by interacting with the particles inside the neutron star. The last factor in eq. (3.3),  $f$ , determines the fraction of the dark matter particles that will be trapped inside the neutron star due to interactions with nucleons, which for  $\sigma_{\chi n} < \sigma_{\text{crit}} = \pi m_n R^2 / M \simeq 2 \times 10^{-45} \text{ cm}^2$ ,  $f$  can be approximated as

$$f = \left\langle 1 - \exp \left[ - \int \frac{\sigma_{\chi n} \rho}{m_n} dl \right] \right\rangle \simeq \left\langle \int \frac{\sigma_{\chi n} \rho}{m_n} dl \right\rangle, \quad (3.4)$$

where  $dl$  is the infinitesimal arc length of a trajectory in the neutron star [16, 26]. Assuming constant density for the neutron star, numerical evaluation of  $f$  in terms of the critical cross section,  $\sigma_{\text{crit}}$ , which is the geometrical cross section of the neutron star divided by the number of nucleon targets, is given by [26]

$$f \simeq \frac{\sigma_{\chi n}}{\sigma_{\text{crit}}} \left\langle \int \frac{\rho}{M/R^3} \frac{dl}{R} \right\rangle \simeq 0.45 \frac{\sigma_{\chi n}}{\sigma_{\text{crit}}}. \quad (3.5)$$

This equation is applicable to the case where  $\sigma_{\chi n} < \sigma_{\text{crit}}$ , however  $f$  saturates to unity when  $\sigma_{\chi n}$  is larger than  $\sigma_{\text{crit}}$  [26]. Thus, the quantity  $f$  is

$$f \simeq 0.45 \frac{\min(\sigma_{\chi n}, \sigma_{\text{crit}})}{\sigma_{\text{crit}}}. \quad (3.6)$$

Currently, the most stringent experimental limits on the DM-nucleon cross section,  $\sigma_{\chi n}$ , come from the XENON [41] and CDMS [42] experiments which look for energy deposition via nuclear recoils from dark matter scattering. For dark matter mass between 20 GeV and 100 GeV, the limit is  $\sigma_{\chi n} < 6 \times 10^{-44} \text{ cm}^2$ , while for larger mass, i.e.  $m_\chi = 10^3 \text{ GeV}$ , the limit is about an order of magnitude larger and similar for lighter dark matter particle, when  $m_\chi \sim 15 \text{ GeV}$ . Recently, CRESST-II has claimed  $4.7\sigma$  signal corresponding to  $m_\chi \sim 10 - 30 \text{ GeV}$  and for  $10^{-40} \text{ cm}^2 < \sigma_{\chi n} < 3 \times 10^{-43} \text{ cm}^2$  [43]. This signal does not seem to be consistent with DAMA results claiming annual modulation effect consistent with dark matter particle of mass around 10 GeV with the cross section  $\sigma_{\chi n} \sim 10^{-40} \text{ cm}^2$  [44]. We will incorporate these limits by taking conservative approach and considering only cases when  $\sigma_{\chi n}$  is below  $10^{-44} \text{ cm}^2$ , written as  $\sigma_{\chi n} = \sigma_{\chi n,55} 10^{-55} \text{ cm}^2$ .

The parameters that we use are given in Table 1. With these parameters, the capture rate,  $C_c$ , for  $\sigma_{\chi n} < \sigma_{\text{crit}} = 2 \times 10^{-45} \text{ cm}^2$ , is given by,

$$C_c = 9.19 \times 10^{22} \frac{\sigma_{\chi n,55}}{m_\chi/\text{GeV}} \frac{\rho_\chi}{\text{GeV}/\text{cm}^3} \xi \text{ yr}^{-1} \quad (3.7)$$

### 3.2 Dark Matter Self Interactions

Once a certain amount of dark matter particles accumulates in the neutron star, their very existence inside the neutron star will affect the capture of new dark matter particles due to their self-interaction [17]. The self-capture rate,  $C_s$ , is given by [17]

$$C_s = \sqrt{\frac{3}{2}} \frac{\rho_\chi}{m_\chi} \sigma_{\chi\chi} v_{\text{esc}}(R) \frac{v_{\text{esc}}(R)}{\bar{v}} \langle \hat{\phi}_\chi \rangle \frac{\text{erf}(\eta)}{\eta} \frac{1}{1 - \frac{2GM}{R}}, \quad (3.8)$$

where,  $\sigma_{\chi\chi}$  is the dark matter elastic scattering cross-section and  $v_{\text{esc}}(R)$  is the escape velocity from the surface of the neutron star. As discussed in Sec. 2.2, it is primarily the gravitational

effect of the neutron star that keeps the dark matter inside the neutron star, eventually thermalizing, so eq. (3.8) depends on the neutron star radius  $R$  rather than the details of the dark matter distribution within the neutron star. We modified eq. (3.8) following Ref. [26] in order to take into account the general relativistic effects assuming as Schwarzschild geometry. The quantity  $\hat{\phi}_\chi$  which signifies how compact the star, is a dimensionless potential defined as [17],

$$\hat{\phi}_\chi = \frac{v_{esc}^2(r)}{v_{esc}^2(R)}. \quad (3.9)$$

We take  $\langle \hat{\phi}_\chi \rangle = 1$ , which is valid in the approximation that the mass density of the neutron star is uniform. Since the density is larger in the core, which implies that  $\langle \hat{\phi}_\chi \rangle > 1$ , our assumption is conservative. Finally,  $\eta^2 \equiv 3/2(v_N/\bar{v})^2$  depends on the velocity of the neutron star  $v_N$  in the Galaxy. We approximate  $\text{erf}(\eta)/\eta \simeq 1$ .

The most stringent limits on self-interaction cross section,  $\sigma_{\chi\chi}$ , come from the Bullet Cluster observations [45], i.e.

$$\frac{\sigma_{\chi\chi}/10^{-24} \text{ cm}^2}{m_\chi/\text{GeV}} < 2, \quad (3.10)$$

so we scale the self interaction cross section,  $\sigma_{\chi\chi} = \sigma_{\chi\chi,24} 10^{-24} \text{ cm}^2$ . With our choice of the parameters given in Table I,  $C_s$  is given by,

$$C_s = 1.06 \times 10^{-3} \frac{\sigma_{\chi\chi,24}}{m_\chi/\text{GeV}} \frac{\rho_\chi}{\text{GeV}/\text{cm}^3} \text{yr}^{-1}. \quad (3.11)$$

The full evolution of  $N_\chi(t)$  depends on how quickly the dark matter thermalizes, and whether or not the geometric limit is reached, before or after thermalization. We first discuss the circumstance where  $t_G < t_{th} < t_{max}$ . As discussed above, the geometric limit for DM capture via  $\chi\chi$  interactions, when  $N_\chi(t_G) < \pi r_\chi^2(t_G)/\sigma_{\chi\chi}$ , halts the exponential increase in DM accumulation. For  $t < t_G$ , eq. (3.1) with  $C_a = 0$ ,

$$\frac{dN_\chi}{dt} = C_c + C_s N_\chi, \quad (3.12)$$

governs the evolution. Between  $t_G < t < t_{th}$ , the equation governing the time evolution of  $N_\chi$  is

$$\begin{aligned} \frac{dN_\chi}{dt} &= C_c + C_s N_\chi(t_G) \times \frac{r_\chi^2(t)}{r_\chi^2(t_G)} \\ &\simeq C_c + C_s N_\chi(t_G) \times \frac{t_G}{t}. \end{aligned} \quad (3.13)$$

The shrinking dark matter sphere accounts for the second term in eq. (3.13). Once the thermalization time is reached, a third phase of dark matter accumulation occurs, with

$$\frac{dN_\chi}{dt} = (C_c + C_s \frac{\pi r_{th}^2}{\sigma_{\chi\chi}}), \quad t_{th} < t < t_{max}. \quad (3.14)$$

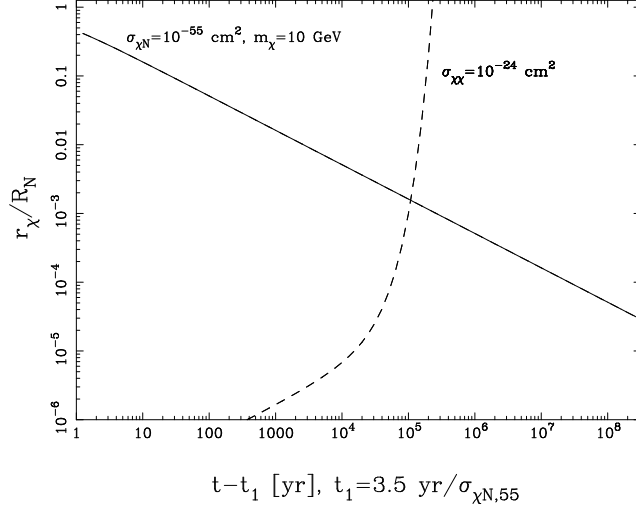


**Figure 3.** As a function of time,  $r_\chi(t)/R$  (solid line) and  $\sqrt{N_\chi^0(t)\sigma_{\chi\chi}/\pi R^2}$  (dashed curve) for  $\sigma_{\chi\chi,24} = 1$  and  $\sigma_{\chi n,55} = 1$ ,  $m_\chi = 10$  GeV and  $\rho_\chi = 1$  GeV/cm<sup>3</sup>. The time at which the solid line and dashed curve cross is  $t_G$ .

The solutions to these equations give the number of dark matter particles at  $t = t_{max}$  of

$$N_\chi(t_{max}) = N_\chi(t_{th}) + \left(C_c + C_s \frac{\pi r_{th}^2}{\sigma_{\chi\chi}}\right)(t_{max} - t_{th}) \quad (3.15)$$

$$N_\chi(t_{th}) = N_\chi(t_G) + C_c(t_{th} - t_G) + C_s N_\chi(t_G) t_G \ln\left(\frac{t_{th}}{t_G}\right) \quad (3.16)$$

$$N_\chi(t_G) = \frac{\pi r_\chi^2(t_G)}{\sigma_{\chi\chi}}. \quad (3.17)$$

As an illustration, we show in Fig. 3 the evolution of  $r_\chi(t)/R$  and  $\sqrt{N_\chi^0(t)\sigma_{\chi\chi}/\pi R^2}$  for  $\sigma_{\chi\chi,24} = 1$  with  $\sigma_{\chi n,55} = 1$  and  $m_\chi = 10$  GeV. The quantity  $N_\chi^0(t)$  is defined in eq. (3.2). We also use  $\rho_\chi = 1$  GeV/cm<sup>3</sup>, equivalent to a distance of  $d = 3.7$  kpc from the Galactic Center for a dark matter density parameterized by the Navarro-Frank-White halo profile [46]. The intersection of lines is  $t_G$ . For  $\sigma_{\chi\chi,24} = 1$ ,  $t_G \simeq 10^5$  yr. The resulting time evolution of  $N_\chi$  for  $\sigma_{\chi\chi,24} = 1$  is shown in Fig. 4.

For other parameters, the time ordering of  $t_G$ ,  $t_{th}$  and  $t_{max}$  can be different. If  $t_{th} < t_G$ ,  $t_{max}$ , then the dark matter sphere decreases to the thermal radius while the number of accumulated dark matter particles follows  $N_\chi^0(t)$ , eq. (3.2). After  $t_{th}$ , at some point  $t'_G$ ,

$$N_\chi(t'_G)\sigma_{\chi\chi} = \pi r_{th}^2. \quad (3.18)$$

when the geometric limit is reached. If  $t'_G > t_{max}$  then

$$N_\chi(t_{max}) = \frac{C_c}{C_s} \left( e^{C_s t_{max}} - 1 \right). \quad (3.19)$$

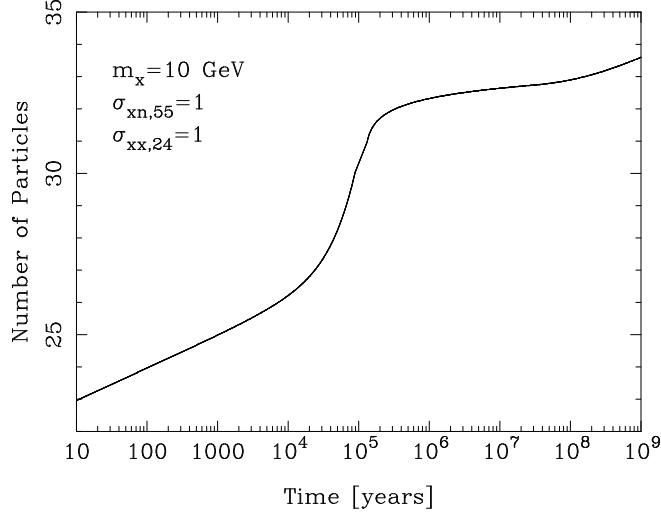


**Figure 4.** As a function of time,  $N_\chi(t)$  for  $\sigma_{\chi\chi,24} = 1$ ,  $\sigma_{\chi n,55} = 1$ ,  $m_\chi = 10$  GeV and  $\rho_\chi = 1$  GeV/cm<sup>3</sup>.

If  $t_{th} < t'_G < t_{max}$  then

$$N_\chi(t_{max}) = \frac{\pi r_{th}^2}{\sigma_{\chi\chi}} + \left( \frac{C_s \pi r_{th}^2}{\sigma_{\chi\chi}} + C_c \right) (t_{max} - t'_G). \quad (3.20)$$

## 4 Results and Discussion

In Figures 5, 6 and 7, we show the time evolution of the number of dark matter particles captured by a neutron star for  $m_\chi = 1$  GeV,  $m_\chi = 10$  GeV and  $m_\chi = 100$  GeV, and for several values of dark matter interaction cross sections. We have taken the Galactic dark matter density to be 1 GeV cm<sup>-3</sup> and other parameters as given in Table 1. The self-interaction cross section is taken to be  $\sigma_{\chi\chi} = 10^{-24}$  cm<sup>2</sup> and we consider two different values for dark matter nucleon interaction cross section,  $\sigma_{\chi n} = 10^{-55}$  cm<sup>2</sup> (top panels of Figs. 4-6) and  $\sigma_{\chi n} = 10^{-48}$  cm<sup>2</sup> (bottom panels of Figs. 5-7). When the dark matter-nucleon cross section is small,  $\sigma_{\chi n} = 10^{-55}$  cm<sup>2</sup>, the dark matter self-capture is important, as shown by the upper solid curve in the top panels of Figs. 5-7. Neglecting self-capture yields the lower dashed lines in the top panels. In the bottom panels,  $\sigma_{\chi n} = 10^{-48}$  cm<sup>2</sup> and the self-capture contribution is negligible compared to the capture by nucleons.

Figs. 5-7 illustrate features of the evolution of  $N_\chi(t)$  for low  $\sigma_{\chi n}$  and large  $\sigma_{\chi\chi}$ . When self-interactions are important, the accumulated dark matter in neutron stars can be several orders of magnitude larger than without self-interactions. Is  $N_\chi(t_{max})$  sufficiently large, with self-interactions, to potentially form a black hole and disrupt the neutron star? For  $m_\chi = 10$  GeV, our minimal limit is  $N_b^{BEC}(r = r_{th}) = 2.7 \times 10^{36}$  for  $T = 10^5$  K, a limit larger by almost three orders of magnitude than  $N_\chi(t_{max})$  when  $\rho_\chi = 1$  GeV/cm<sup>3</sup>. This leads us to consider regions where  $\rho_\chi$  is on the order of  $10^3$  GeV/cm<sup>3</sup>, since to a good approximation,  $N_\chi(t)$  scales linearly with  $\rho_\chi$ .

Assuming that the dark matter density in the Galaxy follows the NFW distribution, it can be seen that regions where the DM density can reach to  $\rho_\chi \sim 10^3$  GeV/cm<sup>3</sup> are very

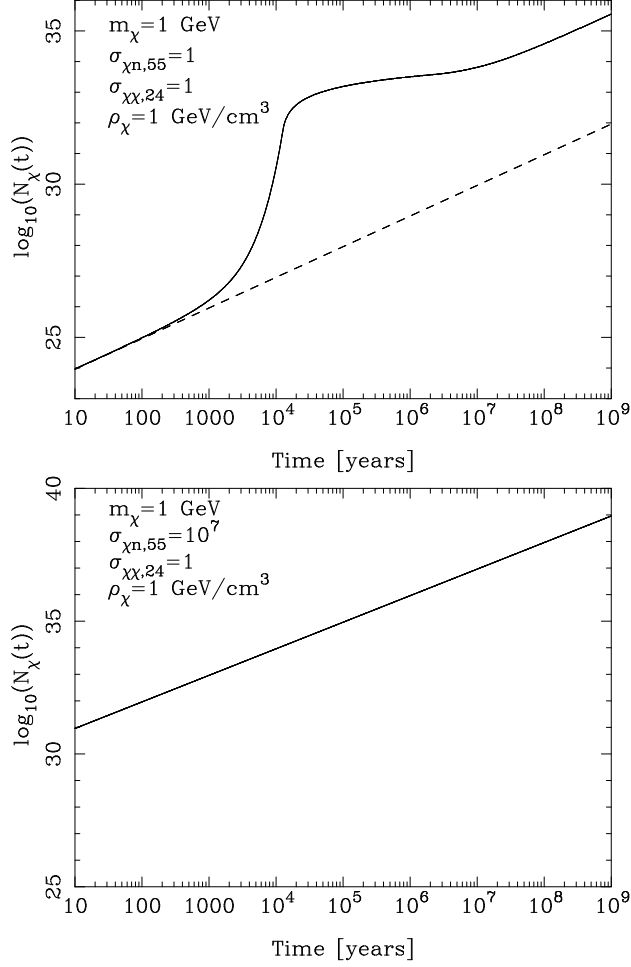


**Figure 5.** Time evolution of the number of asymmetric bosonic dark matter particles accumulated in a neutron star, for  $m_\chi = 1$  GeV,  $\sigma_{\chi\chi} = 10^{-24}$  and  $\sigma_{\chi n} = 10^{-55}$  cm<sup>2</sup> (top panel) and  $\sigma_{\chi n} = 10^{-48}$  cm<sup>2</sup> (bottom panel). The DM density is taken to be  $\rho_\chi = 1$  GeV/cm<sup>3</sup>. The dashed line in the top panel is for  $\sigma_{\chi\chi,24} = 0$ .

limited. However, globular clusters may provide the regions with excessive DM density. It has been shown by Bertone and Fairbairn [21] that within the core radius of the globular cluster M4, the DM density may reach to  $\approx 34,000$  GeV/cm<sup>3</sup>, although the existence of large dark matter densities associated with globular clusters has been controversial [49]. Within the core of this cluster, the well known millisecond pulsar PSR B1620-26 has been detected [47]. This pulsar has a minimum characteristic age of  $2.2 \times 10^8$  yr [48].

Similar to M4, many neutron stars have been discovered in other globular clusters. For example, the globular cluster 47 Tuc has a core radius of 0.6 pc. In the core of the cluster at least 5 neutron stars have been located. In total, within a few times the core radius of this cluster, 20 neutrons stars have been located all with typical minimum characteristic ages of a few  $\times 10^8$  yr [50]. So while  $\rho_\chi = 10^3$  GeV/cm<sup>3</sup> is likely not common, it appears that there might be regions with such high dark matter densities with old neutron stars.

Fig. 8 shows  $\log_{10}(N_\chi(t_{max}))$  and  $\log_{10}(N_\chi(t_G))$  as a function of  $m_\chi$  for  $\rho_\chi = 10^3$  GeV/cm<sup>3</sup>. In this figure, we have chosen  $\sigma_{\chi n,55} = 100$  and  $\sigma_{\chi\chi,24} = 10^{-3}$  and 1, but  $N_\chi(t_{max})$  as a function of  $m_\chi$  is nearly equal to the curve shown in Fig. 8 for a wide range of  $\sigma_{\chi n,55}$

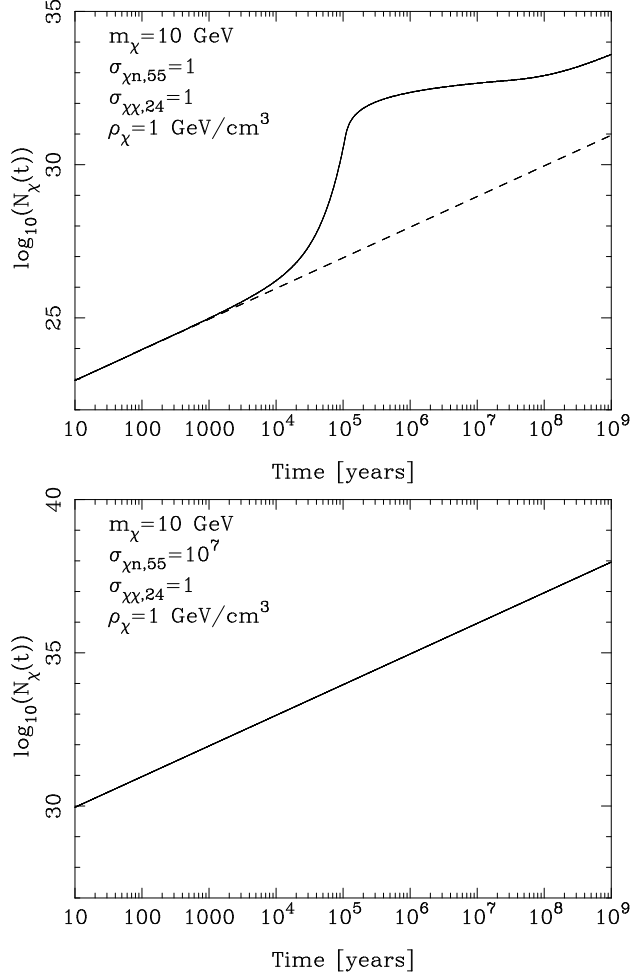


**Figure 6.** Same as Fig. 5, but for  $m_\chi = 10$  GeV.

and  $\sigma_{\chi\chi,24}$ . Whether  $t_G < t_{th}$  or  $t_G > t_{th}$ , for  $t_{max} \gg t_{th}$ , we can approximate eq. (3.15) or eq. (3.20) by

$$N_\chi(t_{max}) \simeq \left( C_c + C_s \frac{\pi r_{th}^2}{\sigma_{\chi\chi}} \right) t_{max}. \quad (4.1)$$

When the term proportional to  $C_s$  is most important, this simplifies to

$$\begin{aligned} N_\chi(t_{max}) &\simeq C_s \frac{\pi r_{th}^2}{\sigma_{\chi\chi}} t_{max} \\ &\simeq 3.5 \times 10^{38} \frac{\text{GeV}^2}{m_\chi^2} \frac{\rho_\chi}{10^3 \text{ GeV/cm}^3} \frac{t_{max}}{10^9 \text{ yr}}, \end{aligned} \quad (4.2)$$

independent of  $\sigma_{\chi\chi}$  and  $\sigma_{\chi n}$ . As an example, for  $m_\chi = 10$  GeV and  $\sigma_{\chi n,55} = 1$ , eq. (4.2) applies to  $\chi\chi$  cross sections in the range of  $\sigma_{\chi\chi} \sim 10^{-33} - 10^{-24} \text{ cm}^2$ . Even when self-capture dominates, eq. (4.2) is modified when  $t_{th}$  or  $t'_G$  is close to  $t_{max}$ . In Fig. 8, this is where the curve for  $N_\chi(t_{max})$  deviates from the power law  $N_\chi(t_{max}) \sim m_\chi^{-2}$ .

For masses below  $m_\chi \simeq 7.4$  GeV, the minimal limit for black hole production is  $1.5 \times 10^{38} \text{ GeV}^2/m_\chi^2$ , while for larger masses, we need  $N_\chi(t_{max}) > N_b^{BEC}(r = r_{th}) = 2.7 \times 10^{36}$  for

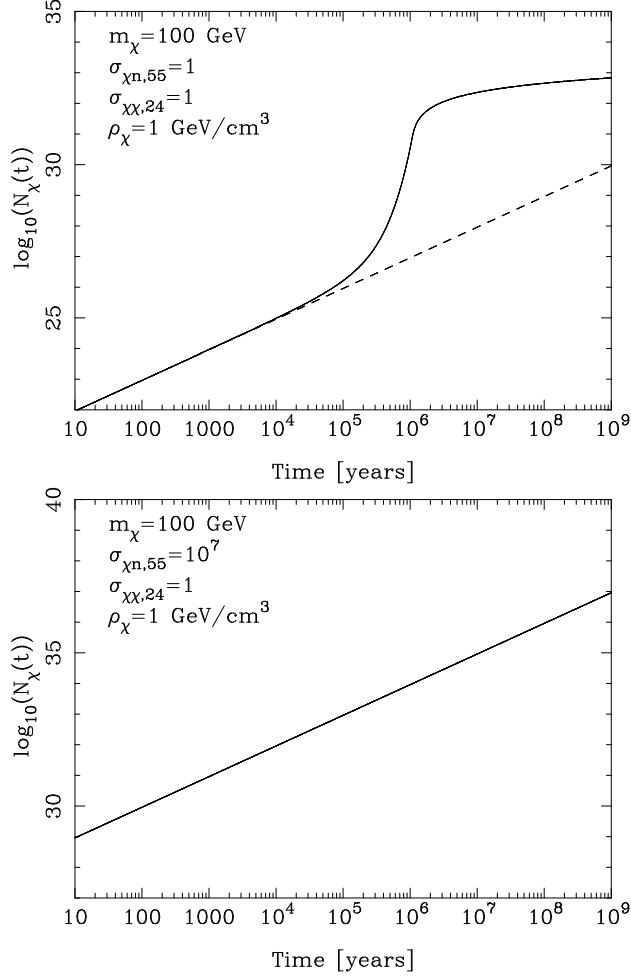


**Figure 7.** Same as Fig. 5, but for  $m_\chi = 100$  GeV.

$T = 10^5$  K. The limits on  $\sigma_{\chi n}$  as a function of mass come from where the solid or dashed lines cross the limits represented by the dotted curve in Fig. 8. Except for the cross sections for  $\chi n$  interactions which have  $t_{th}$  nearly equal to  $t_{max}$ , there is no potential to constrain dark matter masses above approximately  $m_\chi \simeq 13$  GeV, for small  $\chi n$  interactions and large  $\chi\chi$  interactions, even with  $\rho_\chi = 10^3$  GeV/cm<sup>3</sup>.

Our detailed solutions of  $N_\chi(t)$  for  $C_a = 0$ , shown in eqs. (3.15-3.17, 3.19, 3.20), rely on  $r_\chi(t)$  assuming  $\chi n$  scattering is solely responsible for dark matter cooling in the neutron star. Our result in eq. (4.2), that  $N_\chi(t_{max})$  depends only on the thermalization radius, the dark matter density and  $t_{max}$  when  $C_s$  is most important, gives support to our approximate approach. In the regime where  $\chi\chi$  scattering is responsible for DM capture by the neutron star, only a small energy loss by the incident DM is required for capture. However, in the two particle scattering, the net change in energy is zero. For  $\chi n$  scattering, the additional neutron energy is dissipated via  $nn$  interactions among the  $\sim 10^{57}$  neutrons. With  $\chi\chi$  scattering, where, e.g.,  $N_\chi^{Ch} \simeq 10^{36}$  for  $m_\chi = 10$  GeV, the energy loss of the incident  $\chi$  is transferred to the target DM, leading to capture of the incident dark matter but not to evaporation of the target dark matter. A more detailed evaluation of the energetics of  $\chi\chi$  scattering may result in some changes in the time evolution of the radius of the dark matter sphere, however, as long

as  $t_{max} \gg t_{th}$ , those details are not important. In view of our rather pessimistic conclusion that only a limited range of dark matter mass is potentially constrained, even with strongly interacting bosons with  $\rho_\chi \sim 10^3 \text{ GeV/cm}^3$ , a more detailed evaluation of  $r_\chi(t)$  does not seem merited.

## 5 Conclusions

Our limiting results for  $\rho_\chi = 10^3 \text{ GeV/cm}^3$  using  $N_b^{Ch}$  and  $N_b^{BEC}(r = r_{th})$  are shown in Fig. 9. The upper region is excluded when  $\sigma_{\chi\chi} = 0$ , because of  $\chi n$  scattering. Thermalization is crucial for the dark matter particles to become self-gravitating, thus the region of parameter space for which the thermalization does not occur cannot be excluded by considering the collapse of the neutron star. The region labeled “no thermalization” shows the region of parameters for which  $t_{th} > 10^9 \text{ yr}$ . The vertical line in Fig. 9 comes from the Bullet Cluster limit when  $\sigma_{\chi\chi,24} = 1$  in eq. (3.10), namely that  $m_\chi > 0.5 \text{ GeV}$ .

The upper exclusion region in Fig. 9 is consistent with the limits in Ref. [11] for our choice of  $t_{max}$ . This limit takes into account Bose-Einstein condensate. A similar shape for the exclusion region without the Bose-Einstein condensate restriction (for  $m_\chi > 7.4 \text{ GeV}$ ) appears in Ref. [27]. For  $m_\chi < m_n$ , the inclusion of Pauli blocking changes the slope of the limiting exclusion region for  $\sigma_{\chi\chi,24} = 0$ .

In Fig. 9, the middle region shows the potential exclusion range of  $\sigma_{\chi n}$  when  $\sigma_{\chi\chi,24} = 1$  (labeled “excluded  $\sigma_{\chi\chi,24} = 1$ ”). The almost vertical line near  $m_\chi \sim 10 \text{ GeV}$ , beyond which we have no constraints, comes from using  $N_{min} = N_b^{BEC}(r = r_{th})$ , where the dotted line in Fig. 8 crosses the solid line.

While Fig. 9 is only for one choice of  $\sigma_{\chi\chi,24}$ , we found the limits on  $\sigma_{\chi n,55}$  as a function of  $m_\chi$  are applicable for a wide range of  $\sigma_{\chi\chi,24}$ . A range of large  $\chi\chi$  interaction cross sections gives an exponential increase similar to that seen in Figs. 5-7, increasing  $N_\chi$  by several orders of magnitude over the case where  $\sigma_{\chi\chi,24} = 0$ . For  $m_\chi = 10 \text{ GeV}$  and  $\sigma_{\chi n,55} = 100$ , the resulting  $N_\chi(t_{max})$  is the same for  $\sigma_{\chi\chi,24} = 10^{-9} - 1$ , resulting in  $N_\chi(t_{max})$  being larger than  $N_b^{BEC}(r = r_{th})$  and thus corresponding to the exclusion region. Since  $C_c \propto \rho_\chi \sigma_{\chi n}$ , when  $\rho_\chi$  decreases, the region with a potential for exclusion of bosonic dark matter decreases. If  $\rho_\chi$  is smaller than  $10^3 \text{ GeV/cm}^3$  by a factor of  $\sim 2$ , we do not have any new limits on self-interacting asymmetric bosonic dark matter for  $t_{max} = 10^9 \text{ yr}$ , even with the minimal Chandrasekhar limit for bosons. Indeed, by changing any combination of parameters like neutron star temperature, mass, radius, and age ( $t_{max}$ ) and the dark matter velocity dispersion in a way that it would give an overall factor of two reduction in  $N_\chi$  (approximated by eq. (4.2)) the limits we obtain would not apply.

The minimal Chandrasekhar bound for bosons given by eq. (2.6) does not apply in case of perturbative repulsive  $\lambda\phi^4$  models for  $\chi\chi$  self interaction. A repulsive interaction can provide extra pressure and increase the minimum number of dark matter particles required to form a black hole [51]. An example of such constraints appears in, for example, Ref. [27] where the resulting  $\chi\chi$  cross sections excluded by neutron stars are in the range of  $\sigma_{\chi\chi,24} \lesssim 10^{-40}$ . Clearly with the large, nonperturbative cross sections that we considered, the limits are different from a perturbative  $\lambda\phi^4$  model considered in Ref. [27].

Evaporation by a newly formed black hole by Hawking radiation will dominate accretion unless  $N_\chi > N_{BH}^{crit} = 5.7 \times 10^{36} \text{ GeV}/m_\chi$  [27]. We note that  $N_b^{Ch} > N_{BH}^{crit}$  for  $m_\chi < 26 \text{ GeV}$ . The more restrictive self-gravitation limit for BEC,  $N_{min} = N_b^{BEC}(r = r_{th}) = 2.7 \times 10^{36}$  is

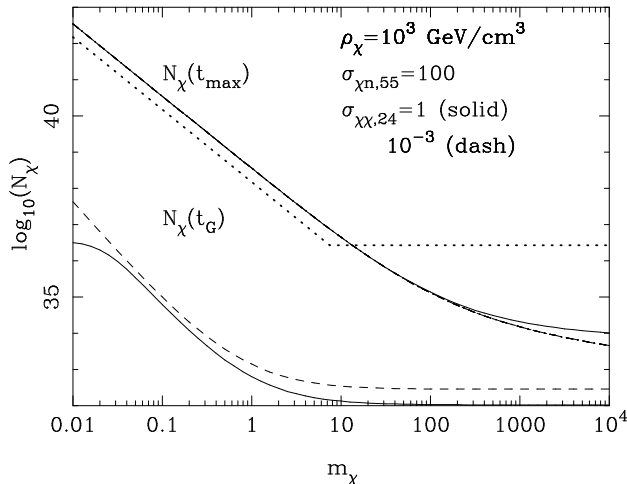


**Figure 8.** As a function of  $m_\chi$ ,  $\log_{10}(N_\chi(t_{max}))$  and  $\log_{10}(N_\chi(t_G))$  for  $\sigma_{\chi n,55} = 100$ ,  $\sigma_{\chi\chi,24} = 10^{-3}$  (dash) and 1 (solid) for  $\rho_\chi = 10^3 \text{ GeV/cm}^3$ . The dotted line shows the limit above which dark matter may collapse to a black hole within the neutron star.

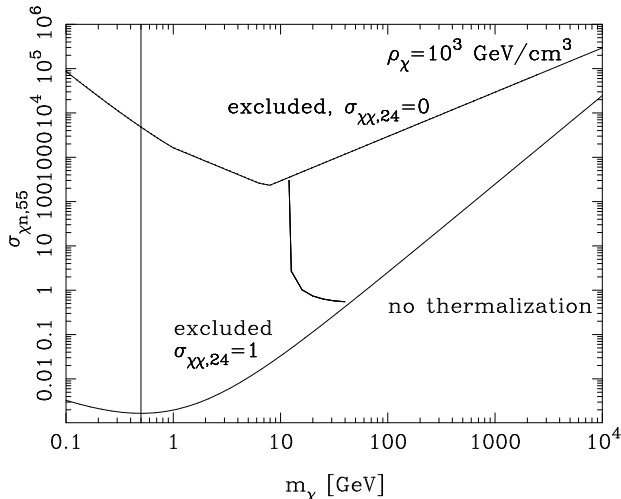


**Figure 9.** As a function of  $m_\chi$ , exclusion regions of  $\sigma_{\chi n,55}$  for  $\sigma_{\chi\chi,24} = 1$  and  $\rho_\chi = 10^3 \text{ GeV/cm}^3$ , using  $N_b^{Ch}$  and  $N_b^{BEC}(r = r_{th})$  for asymmetric bosonic dark matter. The region to the left of the vertical line at  $m_\chi = 0.5 \text{ GeV}$  is excluded by the Bullet Cluster limit when  $\sigma_{\chi\chi,24} = 1$ .

applied when  $7.4 \text{ GeV} < m_\chi < 1.26 \times 10^4 \text{ GeV}$  (the dotted line in Fig. 8). Therefore, for the whole exclusion region in Fig. 9, the Hawking radiation limit  $N_\chi(t_{max}) > N_{BH}^{crit}$  is satisfied.

Dark matter self-interactions can make significant contributions to the accumulation of dark matter in a neutron star when the dark matter density is large,  $\rho \sim 10^3 \text{ GeV}$ . We have evaluated the accumulation including the consequences of a time dependent radius for the dark matter distribution in the neutron star. The quantity  $r_\chi(t)$  in eq. (2.18) follows from approximating the cooling of DM as coming from only dark matter-nucleon scattering. As discussed in Sec. IIB, only small energy losses of DM incident on the neutron star and cloud of captured dark matter are required for capture. The net change in energy in  $\chi\chi$  scattering is zero; the dark matter eventually thermalizes with neutrons.

Our main result for  $t_{max} \gg t_{th}$ , when  $C_c$  can be neglected relative to the self-capture

term, is  $N_\chi(t_{max}) \simeq C_s(\pi r_{th}^2/c_{\chi\chi})t_{max}$  (eq. (4.2)), independent of  $\sigma_{\chi\chi}$ . A more detailed evaluation of the time dependence of  $r_\chi(t)$  including the effect of the energy transfer to the already captured DM particles is beyond the scope of this paper, however, the form of eq. (4.2) for  $N_\chi(t_{max})$  points to a conclusion that a refinement of  $r_\chi(t)$  is unlikely to weaken our limits when  $t_{max} \gg t_{th}$ .

For  $\rho_\chi = 10^3 \text{ GeV/cm}^3$ , we have found a new portion of parameter space that is excluded using  $N_b^{Ch}$  and  $N_b^{BEC}(r = r_{th})$ , for example, the region where the dark matter-nucleon interaction cross section is between  $10^{-52} \text{ cm}^2$  to  $10^{-57} \text{ cm}^2$  and dark matter self-interaction cross section is greater than  $\sim 10^{-33} \text{ cm}^2$  for  $m_\chi = 10 \text{ GeV}$ . As discussed earlier, this region is interesting because thermalization takes a long enough time that self-interactions play a significant role in capturing dark matter particles.

Appreciable dark matter accumulation through self-interactions requires large dark matter densities. For stars in the core of a globular cluster, the dark matter density could be as high as  $10^3 \text{ GeV/cm}^3$  [19]. If the dark matter density is this high and the minimal limits of  $N_b^{Ch}$  and  $N_b^{BEC}(r = r_{th})$  are applicable, the dark matter self-interaction cross section,  $\sigma_{\chi\chi}$ , is constrained when it is in the range between  $10^{-33} \text{ cm}^2$  and  $10^{-24} \text{ cm}^2$ , which is several orders of magnitude more restrictive than the Bullet Cluster limit.

Finally, as we have noted, we have used eq. (2.6) and  $N_b^{BEC}(r = r_{th})$  to constrain bosonic dark matter in neutron stars. Recent work has considered specific models for dark matter self-interactions that rely on perturbation theory, and a parameter space of repulsive couplings is ruled out by the observation of old very old neutron stars [31–33]. A more sophisticated Chandrasekhar limit for bosons would include modifications in the case of strongly interacting bosons, or attractive interactions, for specific models [32, 38, 51]. We have focused on the Chandrasekhar limit with relativistic bosons as the starting point for the study of self-interacting dark matter. Only a limited range of dark matter mass is potentially constrained with this approach, even with strongly interacting bosons and only for  $\rho_\chi \sim 10^3 \text{ GeV/cm}^3$  or larger dark matter densities. An additional interesting possibility of detecting asymmetric dark matter in the minimal self-interacting dark matter model with gamma-rays has been proposed in Ref. [34].

## Acknowledgments

We would like to thank Dimitrios Psaltis, Dennis Zaritsky and Kathryn Zurek for useful discussions. IS would like to thank the Aspen Center for Physics, where part of this work took place. T.G. acknowledges support from Bilim Akademisi - The Science Academy, Turkey under the BAGEP program. This research was supported by US Department of Energy contracts DE-FG02-91ER40664, DE-FG02-04ER41319, DE-FG02-04ER41298, DE-FG03-91ER40662, DE-FG02-13ER41976, and DE-SC0010114.

## References

- [1] F. Zwicky, *Helv. Phys. Acta* **6**, 110 (1933).
- [2] E. Komatsu *et al.* [WMAP Collaboration], *Astrophys. J. Suppl.* **180**, 330 (2009).
- [3] W. J. Percival *et al.* [BOSS Collaboration], *Astrophys. J.* **657**, 51 (2007).
- [4] D. Clowe *et al.*, *Astrophys. J. Lett.* **648**, 109 (2006).
- [5] E. W. Kolb and M. S. Turner, *Front. Phys.* **69**, 1 (1990).

- [6] G. Bertone, D. Hooper, and J. Silk, *Phys. Rept.* **405**, 279 (2005).
- [7] J. L. Feng, *Ann. Rev. Astron. Astrophys.* **48**, 495 (2010).
- [8] D. E. Kaplan, M. A. Luty, and K. M. Zurek, *Phys. Rev. D* **79**, 115016 (2009).
- [9] T. Cohen, D. J. Phalen, A. Pierce, and K. M. Zurek, *Phys. Rev.* **D82**, 056001 (2010).
- [10] Y. Cui, L. Randall, and B. Shuve, *JHEP* **08**, 073 (2011), [1106.4834](#).
- [11] S. D. McDermott, H.-B. Yu, and K. M. Zurek (2011), [arXiv:1103.5472](#).
- [12] A. R. Zentner and A. P. Hearin, *Phys. Rev.* **D84**, 101302 (2011), [1110.5919](#).
- [13] H. Davoudiasl, *Phys. Rev. D* **88**, 095004 (2013) [[arXiv:1308.3473 \[hep-ph\]](#)].
- [14] K. M. Zurek, [arXiv:1308.0338 \[hep-ph\]](#).
- [15] R. Laha and E. Braaten, [arXiv:1311.6386 \[hep-ph\]](#).
- [16] W. H. Press and D. N. Spergel, *Astrophys. J. Lett.* **296**, 679 (1985).
- [17] A. R. Zentner, *Phys. Rev. D* **80**, 063501 (2009).
- [18] C. Kouvaris and P. Tinyakov, *Phys. Rev. D* **82**, 063531 (2010).
- [19] M. McCullough and M. Fairbairn, *Phys. Rev.* **D81**, 083520 (2010).
- [20] I. Goldman and S. Nussinov, *Phys. Rev. D* **40**, 3221 (1989).
- [21] G. Bertone and M. Fairbairn, *Phys. Rev.* **D77**, 043515 (2008), [0709.1485](#).
- [22] F. Sandin and P. Ciarcelluti, *Astropart. Phys.* **32**, 278 (2009) [[arXiv:0809.2942 \[astro-ph\]](#)].
- [23] P. Ciarcelluti and F. Sandin, *Phys. Lett. B* **695**, 19 (2011) [[arXiv:1005.0857 \[astro-ph.HE\]](#)].
- [24] F. Capela, M. Pshirkov and P. Tinyakov, *Phys. Rev. D* **87**, 123524 (2013) [[arXiv:1301.4984 \[astro-ph.CO\]](#)].
- [25] P. Pani and A. Loeb, [arXiv:1401.3025 \[astro-ph.CO\]](#).
- [26] C. Kouvaris, *Phys. Rev. D* **77**, 023006 (2008).
- [27] C. Kouvaris and P. Tinyakov, *Phys. Rev. Lett.* **107**, 091301 (2011).
- [28] C. Kouvaris and P. Tinyakov, *Phys. Rev. D* **83**, 083512 (2011).
- [29] A. de Lavallaz and M. Fairbairn, *Phys. Rev.* **D81**, 123521 (2010), [1004.0629](#).
- [30] C. Kouvaris, *Phys. Rev. Lett.* **108**, 191301 (2012) [[arXiv:1111.4364 \[astro-ph.CO\]](#)].
- [31] J. Bramante, K. Fukushima and J. Kumar, *Phys. Rev. D* **87**, 055012 (2013) [[arXiv:1301.0036 \[hep-ph\]](#)].
- [32] K. Petraki and R. R. Volkas, *Int. J. Mod. Phys. A* **28**, 1330028 (2013) [[arXiv:1305.4939 \[hep-ph\]](#)].
- [33] N. F. Bell, A. Melatos and K. Petraki, *Phys. Rev. D* **87**, 123507 (2013).
- [34] L. Pearce and A. Kusenko, *Phys. Rev. D* **87**, 123531 (2013).
- [35] C. Kouvaris and P. Tinyakov, *Phys. Rev. D* **87**, no. 12, 123537 (2013) [[arXiv:1212.4075 \[astro-ph.HE\]](#), [arXiv:1212.4075 \[astro-ph.HE\]](#)].
- [36] C. Kouvaris, *Adv. High Energy Phys.* **2013**, 856196 (2013) [[arXiv:1308.3222 \[astro-ph.HE\]](#)].
- [37] J. Bramante, K. Fukushima, J. Kumar and E. Stopnitzky, *Phys. Rev. D* **89**, 015010 (2014) [[arXiv:1310.3509 \[hep-ph\]](#)].
- [38] M. Colpi, S. L. Shapiro, and I. Wasserman, *Phys. Rev. Lett.* **57**, 2485 (1986).
- [39] F. V. Kusmartsev, E. W. Mielke, and F. E. Schunck, *Phys. Rev. D* **43**, 3895 (1991).

- [40] R. Ruffini and S. Bonazzola, *Phys. Rev.* **187**, 1767 (1969).
- [41] E. Aprile *et al.* [XENON Collaboration], *Phys. Rev. Lett.* **107**, 131302 (2011).
- [42] Z. Ahmed *et al.* [CDMS-II Collaboration], *Science* **327**, 1619 (2010).
- [43] G. Angloher *et al.* [CRESST-II Collaboration] (2011).
- [44] E. Aprile *et al.* [XENON Collaboration], *Eur. Phys. J.* **C56**, 333 (2008).
- [45] M. Markevitch, A. H. Gonzalez, D. Clowe, A. Vikhlinin, W. Forman, C. Jones, S. Murray, and W. Tucker, *Astrophys. J. Lett.* **606**, 819 (2004).
- [46] J. F. Navarro, C. S. Frenk, and S. D. M. White, *Astrophys. J.* **462**, 563 (1996).
- [47] A. G. Lyne *et al.*, *Nature* **332**, 45 (1987).
- [48] J. McKenna and A. G. Lyne, *Nature* **336**, 226 (1988).
- [49] C. Conroy, A. Loeb and D. Spergel, *Astrophys. J.* **741**, 72 (2011) [arXiv:1010.5783 [astro-ph.GA]].
- [50] P. C. Freire *et al.*, *MNRAS* **326**, 901 (2001).
- [51] E. W. Mielke and F. E. Schunck, *Nucl. Phys.* **B564**, 185 (2000).